

**Emergence of chimeras through induced multistability**Sangeeta Rani Ujjwal,<sup>1</sup> Nirmal Punetha,<sup>2</sup> Awadhesh Prasad,<sup>3</sup> and Ramakrishna Ramaswamy<sup>1</sup><sup>1</sup>*School of Physical Sciences, Jawaharlal Nehru University, New Delhi 110067, India*<sup>2</sup>*Max Planck Institute for the Physics of Complex Systems, Nöthnitzer Straße 38, D-01187 Dresden, Germany*<sup>3</sup>*Department of Physics and Astrophysics, University of Delhi, Delhi 110007, India*

(Received 16 August 2016; revised manuscript received 10 December 2016; published 7 March 2017)

Chimeras, namely coexisting desynchronous and synchronized dynamics, are formed in an ensemble of identically coupled identical chaotic oscillators when the coupling *induces* multiple stable attractors, and further when the basins of the different attractors are intertwined in a complex manner. When there is coupling-induced multistability, an ensemble of identical chaotic oscillators—with global coupling, or also under the influence of common noise or an external drive (chaotic, periodic, or quasiperiodic)—inevitably exhibits chimeric behavior. Induced multistability in the system leads to the formation of distinct subpopulations, one or more of which support synchronized dynamics, while in others the motion is asynchronous or incoherent. We study the mechanism for the emergence of such chimeric states, and we discuss the generality of our results.

DOI: [10.1103/PhysRevE.95.032203](https://doi.org/10.1103/PhysRevE.95.032203)**I. INTRODUCTION**

Chimeras [1,2] are among the more interesting collective states in extended dynamical systems, consisting of coexisting synchronized and desynchronized subpopulations within an ensemble of coupled identical oscillators. Apart from their application to a variety of physical [3,4] and biological [5,6] situations, the robustness of such complexity has attracted considerable recent interest. Earlier studies have suggested that in order to observe chimera states, some degree of nonuniformity is essential [7], and this nonuniformity can arise due to heterogeneities in the coupling [1,8–10], in the topology [11,12], parameters [13–15], or by allowing for amplitude variation [16]. It has also been seen that time-delay coupling can cause nonuniformity, although it is possible that chimera states reported in several theoretical studies are long transients [17,18].

For such a collective state to occur, it is clear that a necessary (but not sufficient) condition is that the dynamics in the coupled system show multistability [9,19]. The nature of the asymptotic states is of importance—a chimera consists of both coherent and incoherent dynamics, and thus it is important that some of the multistable attractors should lie in the synchronization manifold [20]. An additional requirement is that the symmetry-breaking that leads to different asymptotic states be robust. The dynamics should therefore show final-state sensitivity [21], with the basins of the different attractors being intertwined in a complex manner. A consequence of a complicated basin structure is that in such situations, arbitrary initial conditions will lead to a chimeric state.

In the present work, we build upon the above themes and describe the occurrence of chimeric dynamics in an ensemble of identical chaotic oscillators that are identically coupled without time delay. Multistability is induced in the system through the coupling, and furthermore, the basins of the different coexisting chaotic attractors have a complex structure that ensures the existence of robust chimeras for arbitrary initial conditions. Moreover, if the evolution equations of the system are equivariant, the system can exhibit richer dynamics, e.g., symmetric attractors with in- or out-of-phase dynamics may coexist.

Although the phase space of the system is of dimension  $3N$  (where  $N$  is the number of oscillators in the ensemble), it is useful to utilize a “single-oscillator” description since the projections of the global attractor onto subspaces spanned by each of the individual oscillators remain close to (or very similar to) the attractors in an isolated oscillator. The chimera states—in particular the coherent or incoherent dynamics—are thus with reference to this single-oscillator picture.

The general principles enunciated above can be illustrated in an ensemble of globally coupled Lorenz oscillators [22], although, as will be evident, the results apply quite generally. The mechanism is robust and leads to chimeras in any system wherein stable fixed point(s) and chaotic attractor(s) coexist; this is fairly common, particularly when the systems have symmetries. The emergence of the chimeric state is a consequence of multistability that is *induced* in the system via the direct or indirect interaction of the components. This interaction effectively changes the parameters of the system, leading to multistable dynamics and, therefore, to the creation of the chimeras. Furthermore, the global coupling is unnecessary: it is possible to obtain chimeric states under the influence of a common external modulation [23,24], or with common external noise.

The emergence of chimeras in the system of globally coupled chaotic oscillators is discussed in the next section. The dynamics and existence of chimeric behavior when an ensemble of uncoupled chaotic oscillators is subjected to an external influence are described in Sec. II A. The mechanism of induced multistability and the emergence of chimeras are discussed in Sec. II B. The results obtained for Lorenz oscillators can be generalized in a straightforward manner, and this is illustrated for coupled triple-scroll Chua oscillators in Sec. III. Finally, we summarize the results and discuss the generality and applicability of the findings in Sec. IV.

**II. GLOBALLY COUPLED OSCILLATORS**

Consider an ensemble of  $N$  globally coupled identical Lorenz oscillators with linear diffusive coupling. The dynam-

ical equations are

$$\begin{aligned} \dot{x}_i &= \sigma(y_i - x_i), \\ \dot{y}_i &= rx_i - y_i - x_iz_i, \\ \dot{z}_i &= x_iz_i - \beta z_i + \frac{K}{(N-1)} \sum_{j \neq i} (z_j - z_i), \end{aligned} \quad (1)$$

where  $i, j = 1, \dots, N$  label the oscillators and  $K$  is the strength of mutual coupling. The Lorenz system is equivariant: the flow is invariant under the transformation  $(x, y, z) \rightarrow (-x, -y, z)$ , and this symmetry is evident in the dynamics.

We take the parameters at the standard values,  $\sigma = 10, \beta = 8/3$ . As is well known [25,26], below the subcritical Hopf bifurcation, for  $r \in [24.06, 24.74]$  there are three coexisting attractors: two symmetric fixed points given by  $(\pm \sqrt{\beta(r-1)}, \pm \sqrt{\beta(r-1)}, (r-1))$  along with a strange chaotic attractor.

Consider a value of  $r$  that is above the Hopf bifurcation. The fixed points are unstable, and thus in each isolated Lorenz system (namely for  $K = 0$ ) the dynamics is on a chaotic attractor. On coupling, though, the network of globally coupled oscillators has multiple attractors with different dynamics coexisting in the system: the collective dynamics of Eq. (1) is a chimera, as can be seen in Fig. 1(a) for  $K = 0.07$  for  $r = 24.8$ .

This chimera consists of three distinct subpopulations corresponding to the three attractors of the Lorenz system *below* the Hopf bifurcation. We term these  $B_0$ ,  $B_-$ , and  $B_+$ . In the latter two groups the oscillators are synchronized, while the oscillators in the first group are desynchronized. The chimera in Fig. 1(a), for an ensemble of 100 oscillators, has about 40 oscillators in  $B_-$  and  $B_+$  and the remaining oscillators are in the desynchronized group,  $B_0$ . The  $B_+$  and  $B_-$  groups can have either in-phase or antiphase synchrony between them. This is shown in Fig. 1(b) where the time courses of two randomly selected oscillators from each group,  $B_-$ ,  $B_+$ , and  $B_0$ , are plotted. It should be noted that the type of chimera observed here is different from the chimera states observed in the case of spatially distributed nonlocally coupled oscillators where the synchronized oscillators are localized and are adjacent to each other [1,2,10]. In our case, the spatial coordinates are not important, and depending upon the initial condition an oscillator can go to any of the available attractors, hence several chimera configurations are possible. For clarity of presentation while plotting Fig. 1(a), the oscillator indices are renumbered in such a way that oscillators going to the same attractor are grouped together.

To describe the attractors in various groups, it is convenient to examine the projection of the dynamics onto the  $(x_i, y_i)$  planes. For  $B_0$ , the motion of each oscillator is on a chaotic attractor of the Lorenz type [22,26]. The attractors in  $B_{\pm}$  are also chaotic, but these are stable in the sense that the conditional Lyapunov exponent is negative, and thus the motions of all oscillators in these sets are coherent and synchronized.

An examination of the morphology of the attractors in  $B_{\pm}$  suggests that they are formed via the chaotic modulation of the fixed points  $C_{\pm}$  [25]. The individual oscillators in the ensemble can be considered to be under the influence of a chaotic mean

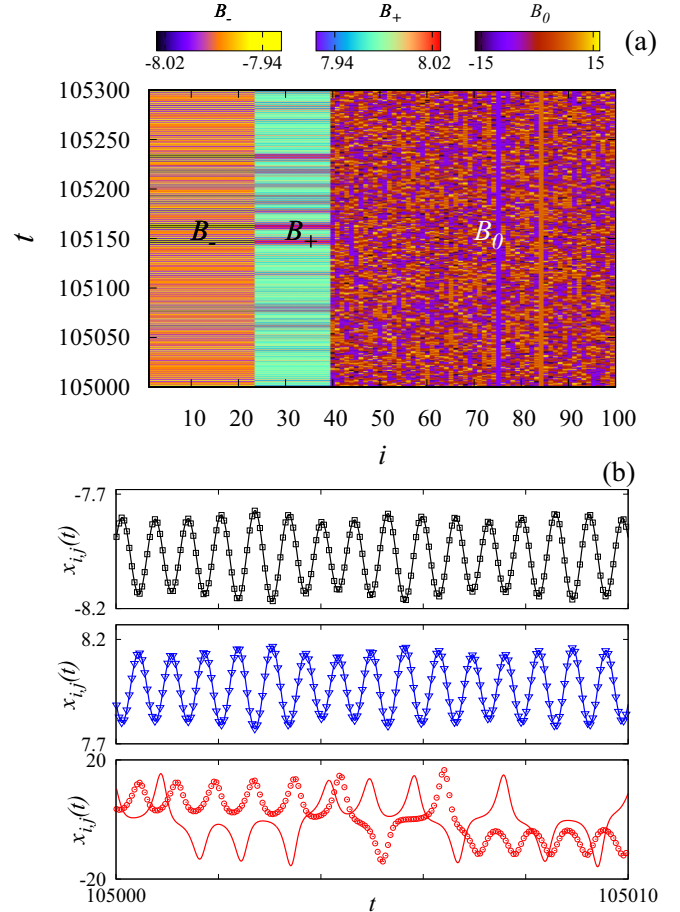


FIG. 1. A chimera for an ensemble of globally coupled Lorenz oscillators [Eq. (1)]: (a) the time evolution of the  $x$ -variable of  $N = 100$  oscillators at parameters  $r = 24.8, \sigma = 10, \beta = 8/3$ , and  $K = 0.07$  starting from random initial conditions  $x_0, y_0, z_0 \in [-100, 100]$ , and (b) time series of the  $x$ -variable,  $x_{i,j}(t)$ , of two arbitrarily chosen oscillators  $i$  and  $j$  (solid line and symbol, respectively) from each group  $B_-$  (upper panel),  $B_+$  (middle panel), and  $B_0$  (lower panel) are plotted.

field given by

$$\bar{f}_m(t) = \frac{1}{(N-1)} \sum_j z_j(t), \quad (2)$$

and thus one can consider the effectively driven system [cf. Eq. (1)]

$$\dot{z}_i = x_iz_i - (\beta + K)z_i + K\bar{f}_m(t), \quad (3)$$

where the time dependence of the mean field is explicitly indicated. Note that this driving preserves the symmetry of the individual Lorenz systems since it affects the  $z$  variables. In the above equation, we observe that parameter  $\beta$  is effectively modified to a value  $\beta + K$ . An additional change in the value of  $\beta$  appears due to the similarity between the mean field  $\bar{f}_m(t)$  and the signal of an isolated unit  $z_i$ . To understand this correction intuitively, we write the mean-field term as  $\bar{f}_m(t) = c_1 z_i(t) + c_0(t)$ . Here,  $c_1$  depends upon the similarity between the mean field and  $z_i$  (which grows with  $K$ ), whereas  $c_0(t)$  can be considered as time-dependent fluctuations. Hence Eq. (3)

can be written as

$$\dot{z}_i = x_i y_i - \bar{\beta} z_i + K c_0(t), \quad (4)$$

where  $\bar{\beta} = \beta + K - c_1 K$ . For mutually coupled system, the correlation between the oscillators grows with the coupling, and synchronization is established in the system above a critical value of  $K > K_{\text{sync}}$ , where all  $x_i, y_i, z_i$ ,  $i = 1, \dots, N$ , are equal.

Consider the fully synchronized system ( $K > K_{\text{sync}}$ ) for example, where  $\tilde{f}_m(t) = z_i(t)$ , i.e.,  $c_1 = 1, c_0 = 0 \Rightarrow \bar{\beta} = \beta$ . This indicates that synchronized motion takes place in a space where the dynamics is similar to the chaotic Lorenz attractor with unaffected parameter values. For  $K < K_{\text{sync}}$ , the effective modification in the parameter in the mutually coupled system is given by  $\bar{\beta} = \beta + K - c_1 K$ . However, for the case of externally modulated systems, where there is no similarity between the drive and response signals—ensemble of oscillators under the influence of a common noise, for example—the values  $c_1 = 0, c_0 = f(t)$ . This implies that the effective parameter is given by  $\bar{\beta} = \beta + \varepsilon$ ; we discuss this case in detail in the following section.

An important effect of the mean-field coupling is that the basins of attraction of the coexisting attractors become complex. Although this is not easily demonstrated for the ensemble of coupled Lorenz oscillators due to the high dimensionality, a study of two coupled Lorenz oscillators gives some indication. For the case of  $r = 28$ , Camargo, Viana, and Anteneodo [27] showed that there were two attractors (in- and out-of-phase) with intermingled basins of attraction that were riddled for sufficiently large coupling. A more detailed analysis of two coupled Lorenz attractors with  $r$  near the Hopf boundary [28] shows that there are several chaotic attractors with complicated basins. It is plausible, therefore, that the basins of the various attractors in the ensemble are strongly mixed, and the basic mechanism for the emergence of chimeric states traces its origin to this feature of the coupled system.

Viewing the coupled system as a set of uncoupled oscillators subject to a common mean-field drive has some parallels with the phenomenon of generalized synchronization [16,29,30]. It is more convenient, therefore, to discuss the emergence of chimeras in an ensemble of forced oscillators, and we turn to this case next.

### A. External modulation

Consider an ensemble of  $N$  Lorenz oscillators driven diffusively by an external signal  $f(t)$  that couples to the variables  $z_j$  as follows:

$$\dot{z}_i = x_i y_i - \beta z_i + \varepsilon [f(t) - z_i], \quad i = 1, \dots, N, \quad (5)$$

where  $\varepsilon$  is the coupling strength (the equations for  $\dot{x}_i$  and  $\dot{y}_i$  are unaffected).

For a chaotic Lorenz system, the mean field, being the superposition of a large number of chaotic signals, is very noisy. When the external signal  $f(t)$  is Gaussian white noise, the asymptotic state of the above system is also chimeric, with the ensemble splitting into three clusters, two of which are synchronized and with one asynchronous cluster, very similar to the case discussed earlier in Sec. II. Results are shown in Fig. 2(a) for  $r = 28$ , with  $N = 100$  oscillators; about 41

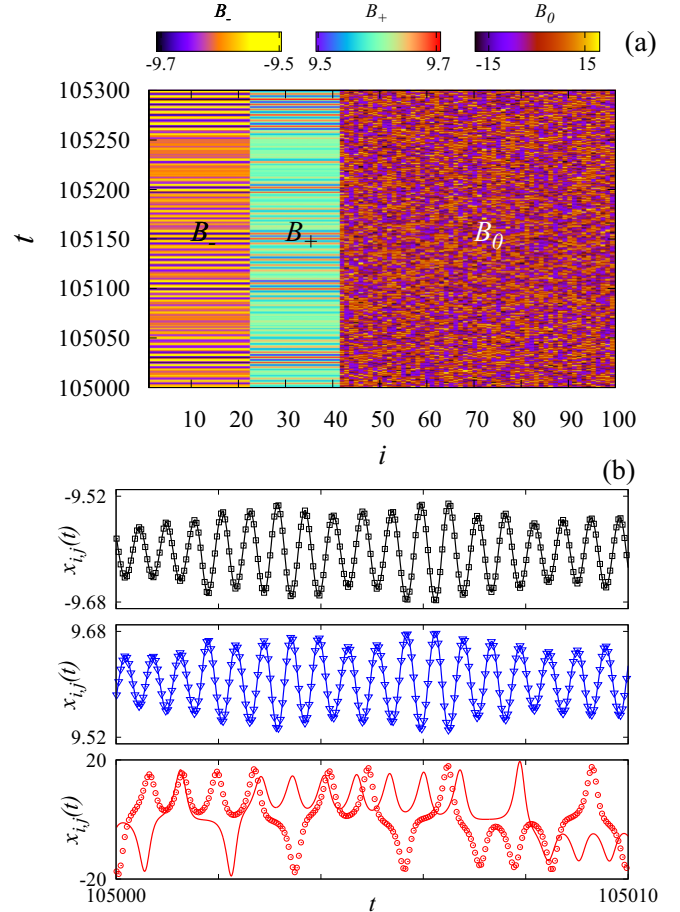


FIG. 2. (a) The time evolution of  $x$ -variables of  $N = 100$  oscillators driven by common Gaussian noise with coupling strength  $\varepsilon = 0.75$  and for  $r = 28$  [Eq. (5)] starting from random initial conditions  $x_0, y_0, z_0 \in [-100, 100]$ . The marked blocks  $B_-$ ,  $B_+$ , and  $B_0$  represent the synchronized groups of attractors  $A_-$ ,  $A_+$ , and desynchronized attractors  $A_0$  of Fig. 3, respectively. (b) Time series of the  $x$ -variable,  $x_{i,j}(t)$ , of two arbitrarily chosen oscillators  $i$  and  $j$  (solid line and symbol, respectively) from each group  $B_-$  (upper panel),  $B_+$  (middle panel), and  $B_0$  (lower panel) are plotted.

oscillators form a synchronized group (blocks  $B_-$  and  $B_+$ ), and the remaining oscillators are desynchronized (block  $B_0$ ). Further, the dynamics of the oscillators in  $B_-$  and  $B_+$  are antiphase to each other, as can be seen in the time-series plots in the upper and middle panels of Fig. 2(b). The oscillators from synchronized blocks  $B_-$  and  $B_+$  correspond to the attractors  $A_-$  and  $A_+$ , respectively, shown in Fig. 3. The desynchronized oscillators in block  $B_0$  are on attractors similar to that of the uncoupled system, namely  $A_0$ . The expanded views of  $A_-$  and  $A_+$  for a noisy drive are shown in the insets in the top left and right panels, respectively.

As may be anticipated, other external drives coupled diffusively will also give very similar asymptotic states, with two coherent clusters and one incoherent one. The basic difference that occurs when the drive is changed is that the dynamics on the attractors ( $A_-$  and  $A_+$ ) that form the coherent clusters changes: A chaotic drive gives rise to chaotic attractors (C), a quasiperiodic drive results in quasiperiodic attractors

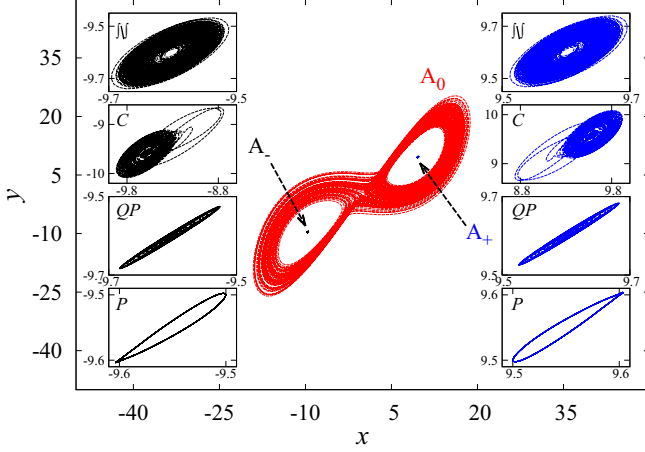


FIG. 3. The trajectories of out-of-phase synchronized attractors,  $A_-$  and  $A_+$ , and desynchronized attractors,  $A_0$ . The left and right panels of the insets show the expanded view of  $A_-$  and  $A_+$ , respectively. Symbols  $\mathcal{N}$ ,  $C$ ,  $QP$ , and  $P$  represent the attractors resulting from the noisy, chaotic, quasiperiodic, and periodic drives, respectively. The chaotic and periodic signals,  $f(t)$ , are taken from chaotic Rössler oscillator ( $a = b = 0.2$  and  $c = 5.7$ ) [31] or the periodic ( $a = b = 0.2$  and  $c = 2$ ) regimes, respectively. For a quasiperiodic drive, we take  $f(t) = \cos(a_1 t) + \cos(a_2 t)$ , where  $a_1 = 1$  and  $a_2 = 0.5(1 + \sqrt{5})$ . The driving strength  $\varepsilon = 0.75$  for all cases.

( $QP$ ), and a periodic drive gives rise to periodic attractors ( $P$ ). These are shown in the left and right panels of the insets in Fig. 3, while the structure of the desynchronized attractor  $A_0$  does not change under any of the different drives. The attractors observed in the case of a chaotic drive are similar to the one observed in earlier works [24] when the drive is a chaotic signal from a Rössler oscillator.

The structure of the chimeras observed when an ensemble of identical chaotic oscillators is subjected to chaotic, quasiperiodic, and periodic external drives is shown in Fig. 4. Note that unlike the case of globally coupled oscillators, the parameter values of the individual Lorenz oscillators can be quite far from the Hopf boundary, and the coupling can still drive the system into a chimera state by effectively creating multistability in the dynamics of each oscillator. The mechanism is explored below.

### B. Coupling-induced multistability

For simplicity, we first discuss the effect of external driving on a single Lorenz oscillator [cf. Eq. (5)], for which the dynamical equations can be rewritten as

$$\begin{aligned} \dot{x} &= \sigma(y - x), \\ \dot{y} &= rx - y - xz, \\ \dot{z} &= xy - \bar{\beta}z + \varepsilon f(t), \end{aligned} \quad (6)$$

where  $\bar{\beta} = (\beta + \varepsilon)$ . The system given in Eq. (6) can be interpreted as a modified Lorenz oscillator ( $L'$ ) with parameter  $\bar{\beta}$  that is driven by an external signal  $\varepsilon f(t)$ . Recall that the unforced Lorenz system ( $\varepsilon = 0$ ) has two symmetric fixed points that coexist with the strange attractor  $A_0$  for

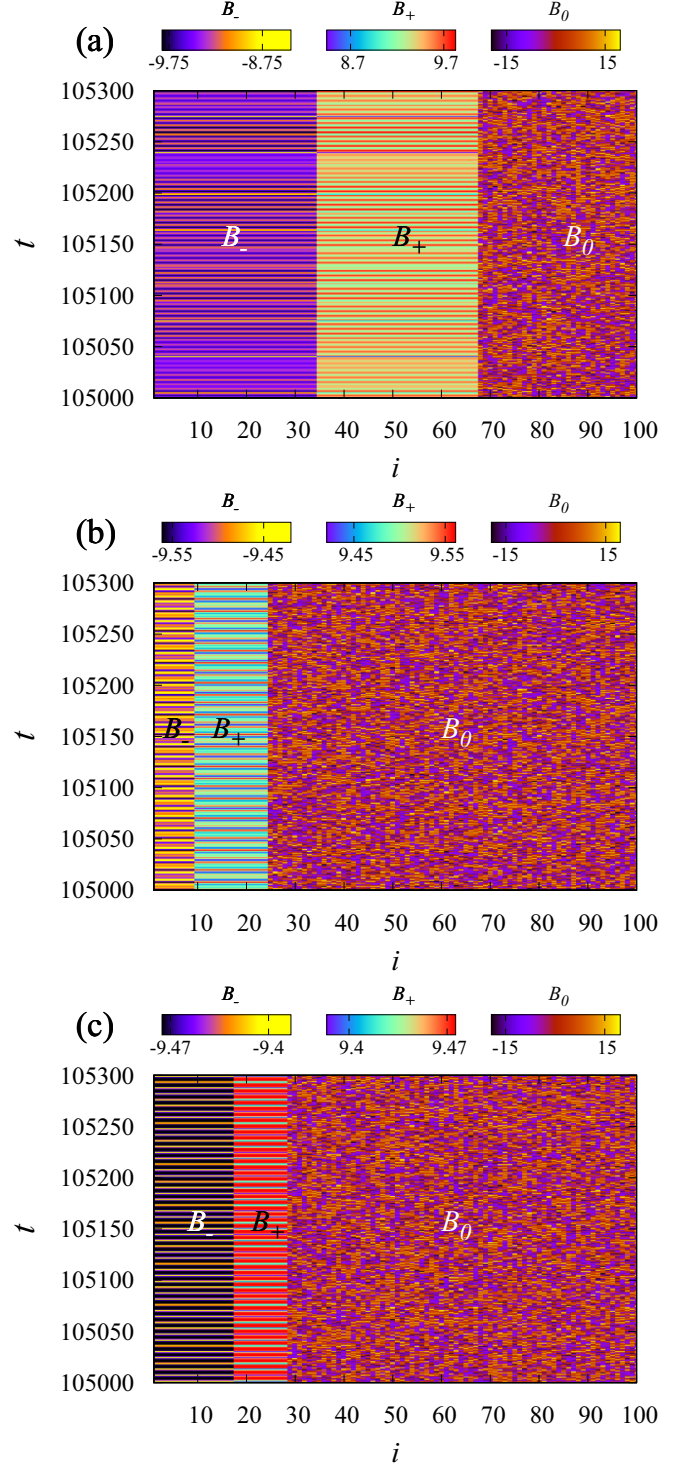


FIG. 4. Plots similar to Fig. 1 showing the existence of chimeras for  $N = 100$  oscillators driven by (a) a chaotic signal [31] of strength  $\varepsilon = 0.65$ , (b) a quasiperiodic signal of strength  $\varepsilon = 0.66$ , and (c) a periodic signal of strength  $\varepsilon = 0.66$ . The oscillators in the two synchronized groups ( $B_-$  and  $B_+$ ) settle onto attractors  $A_-$  and  $A_+$ , respectively, whereas the dynamics of oscillators in the desynchronized group ( $B_0$ ) lie on the strange attractor,  $A_0$  (see Fig. 3).

appropriate values of  $\sigma$ ,  $r$ , and  $\beta$ . By varying  $\varepsilon$ , the system ( $L'$ ) is driven into a regime where the fixed points  $C_{\pm}^* \equiv (\pm\sqrt{\bar{\beta}(r-1)}, \pm\sqrt{\bar{\beta}(r-1)}, (r-1))$  are stable, and they co-

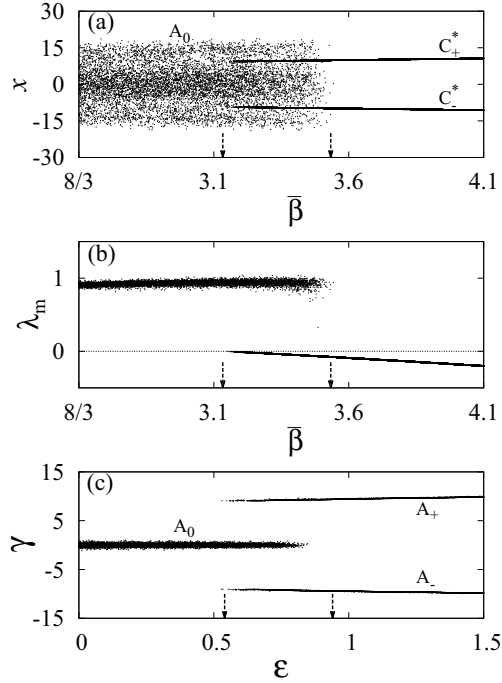


FIG. 5. (a) Bifurcation-type diagram and (b) the largest Lyapunov exponent with parameter  $\tilde{\beta}$  of a modified Lorenz system  $L'$ . (c) The order parameter  $\gamma$  is plotted with the coupling strength  $\epsilon$  for Eq. (5) for 10 initial conditions. For different initial conditions, the three branches in (c) correspond to the oscillator going to three different attractors  $A_0$ ,  $A_-$ , and  $A_+$  of Fig. 3. The correspondence between the stabilization of the fixed points  $C_{\pm}^*$  of a modified Lorenz system  $L'$  [(a) and (b)] and the appearance of the attractors  $A_{\pm}$  in system (5) [(c)] can be observed. Multistability exists in the parameter region marked with the arrows.

exist alongside the chaotic attractor  $A_0$ . Of course since the system is driven, the fixed points are transformed into attractors so that one observes two synchronous attractors  $A_{\pm}$ : the common external drive  $\epsilon f(t)$  does not affect the intrinsic stability of the fixed points.

As can be seen in Fig. 5, there is a direct correspondence between the appearance of the fixed points  $C_{\pm}^*$  in  $L'$  [Eq. (6) with  $f(t) = 0$ ] as a function of  $\tilde{\beta}$  and that of the attractors  $A_{\pm}$  in the ensemble Eq. (6) as a function of driving strength  $\epsilon$ . In Fig. 5(a) the bifurcation diagram is plotted, and in Fig. 5(b) we plot the largest Lyapunov exponent of the modified system ( $L'$ ) as a function of  $\tilde{\beta}$ . These diagrams clearly show that two stable fixed points  $C_{\pm}^*$  coexist along with the chaotic attractor  $A_0$  for sufficiently large  $\tilde{\beta}$ .

The quantity  $\gamma = (x_{\max} + x_{\min})/2$  for each of the attractors, and it is plotted in Fig. 5(c) (estimated for 100 initial conditions at each  $\epsilon$  value) as a function of coupling strength  $\epsilon$  for  $f(t)$  taken to be Gaussian noise. The different values of  $\gamma$  indicate the attractors  $A_-$ ,  $A_+$  [ $\gamma \approx \sqrt{\tilde{\beta}(r-1)}$ ], or  $A_0$  ( $\gamma \approx 0$ ) onto which the dynamics asymptotically settles for a given initial condition. As can be seen in Fig. 5, there is a parameter range (shown by the arrows) for which  $\gamma$  can take all three types of values, and this is the range of  $\epsilon$  for which chimeras can be observed. For an ensemble of oscillators, we note that whenever the oscillators settle into

the smaller attractors  $A_{\pm}$ , their motions are synchronized due to the common influence, while trajectories asymptoting to the attractor  $A_0$  are incoherent.

Similar behavior is observed for other  $r$  and for other forms of  $f(t)$ , and this is the basic mechanism through which a common external influence brings each system into a multistable regime, and it induces chimeras in the ensemble. In the region where the attractors  $A_{\pm}$  and  $A_0$  coexist, the system may settle into any of the attractors according to their basin of attraction. In this way, a common external signal coupled diffusely can induce multistable behavior in an ensemble of identical oscillators. Then it is inevitable that the oscillators in such an ensemble starting from different initial conditions settle into different attractors, resulting in the identical groups splitting into desynchronized and synchronized clusters and exhibiting chimeric behavior [32]. However, from numerical analysis we note that, at  $r = 28$ , this multistability is not observed when a Lorenz system is driven by the signal of another Lorenz oscillator. This suggests that this behavior also depends upon the nature of the external signal, specifically its similarity with that of the response system. Intuitively, this can be understood from Eq. (4) because the amount of modification in  $\beta$  in this case ( $c_1 \approx 1 \Rightarrow \tilde{\beta} = \beta + \epsilon - c_1\epsilon$ ) is not as much as in the case when two signals (drive and response) are entirely different ( $c_1 = 0 \Rightarrow \tilde{\beta} = \beta + \epsilon$ ).

The mechanism for induced multistability in the case of global coupling can be understood in a similar manner. However, in addition to synchronized attractors appearing due to the fixed points  $A_{\mp}$ , the systems can also exhibit other attractors,  $A_{1,2}$ , similar to the ones discussed by Camargo *et al.* [27] on which the dynamics is synchronized. A figure similar to Fig. 5 is plotted for the case of global coupling (see Fig. 6), where a modified order parameter  $\gamma_m$  is used to detect different dynamics observed in the mutually coupled oscillators:  $\gamma_m = \gamma + \gamma'$ , where  $\gamma' = +1, -1, 0$  for in-phase, antiphase, and desynchronized states, respectively.

### C. Basins of attraction

Given that the chimeras emerge due to the coexistence of multiple attractors, it is natural to investigate the nature of the basins of these different attractors. To study the effect of coupling on the basins of different attractors, we consider the case of two mutually coupled Lorenz oscillators below the Hopf bifurcation point. Figure 7(a) is plotted for  $r = 24.4$  and  $K = 0$  when the system has three stable solutions, namely a strange attractor (cyan) and two symmetric fixed (blue and red) points, with the boundaries of the basins of attraction being smooth. However, for finite coupling,  $K = 0.05$ , the basins of attraction are intertwined, as shown in Fig. 7(b).

In the coupled system, the basin structure of the different attractors is complex [33]: there is a finite probability that two randomly selected nearby initial conditions will asymptote to different attractors ( $A_{\mp}$  and  $A_0$ ). The measured uncertainty exponent lies close to zero, suggesting that the basins are effectively riddled (figure not shown here), but measures such as the transverse Lyapunov exponent and scaling laws [27] have not been straightforward to calculate. Thus while it appears that the basins of the three attractors are intertwined on all scales, the occurrence of riddling has been difficult to

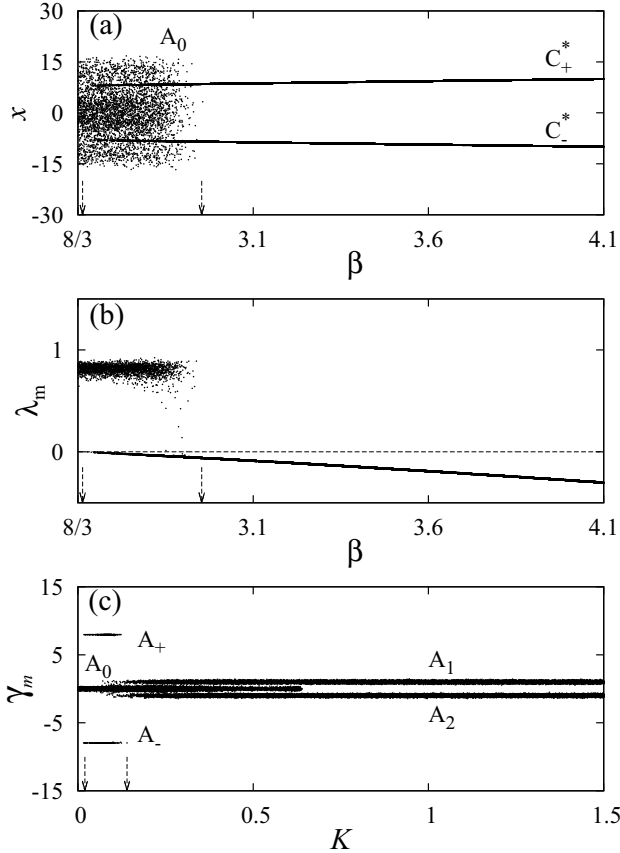


FIG. 6. (a) Bifurcation-type diagram and (b) the largest Lyapunov exponent with parameter  $\beta$  of an isolated Lorenz system at  $r = 24.8$ . (c) The order parameter  $\gamma_m$  is plotted with the coupling strength,  $K$ , for Eq. (1) for 10 initial conditions. For different initial conditions, the five branches in (c) correspond to the oscillator going to different attractors  $A_0$  (desynchronized attractor),  $A_{\pm}$  (attractors appearing due to the fixed points), and  $A_{1,2}$  (in-phase and antiphase synchronized motion in Lorenz attractor).

establish conclusively. The basin structure becomes even more complex for larger  $N$  [28].

It should be noted that even when the basins of different coexisting attractors are well-separated and with distinct boundaries [such as, for example, in Fig. 7(a)], one can get chimeras for random initial conditions. For a careful choice—tightly selected initial conditions that all lie in the basin of a single attractor, for instance—one can get a completely coherent ensemble. However, when the basins become intertwined [as in Fig. 7(b)], it is essentially impossible to avoid the chimera state. We also note that intermixing of basins of attraction of different attractors is important because it can give rise to chimeras for randomly chosen initial conditions even for small system sizes. This can facilitate the observation of chimeras in experimental setups where systems with a large number of oscillators are difficult to realize.

### III. APPLICATION TO THE THREE-SCROLL CHUA SYSTEM

The general scheme described in the previous sections can be extended to a wide variety of nonlinear dynamical

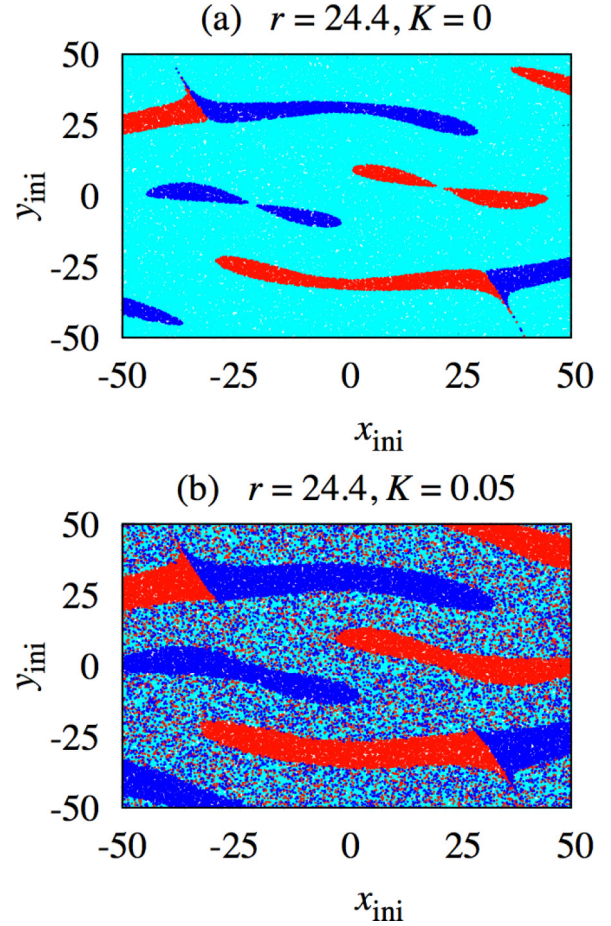


FIG. 7. The basin of attraction of system (1) for parameter values  $r = 24.4$ ,  $\sigma = 10$ , and  $\beta = 8/3$  at mutual coupling strength  $K = 0$  (a) and  $K = 0.05$  (b). The blue (dark gray) and red (medium gray) regions correspond to the basins of smaller attractors  $A_{\pm}$ , while cyan (light gray) corresponds to that of larger attractor  $A_0$ .

systems since the basic features that are required are in fact quite common. For instance, in the two- or multiscroll Chua oscillator, chimera states can essentially be designed as follows.

The dynamical equations for an ensemble of globally coupled Chua oscillators with three scrolls [34] can be written as

$$\begin{aligned} \dot{x}_i &= \alpha[y_i - h_a(x_i, z_i)], \\ \dot{y}_i &= x_i - \rho y_i + z_i + \frac{K}{(N-1)} \sum_{j \neq i} (y_j - y_i), \\ \dot{z}_i &= -\delta y_i, \quad i = 1, \dots, N, \end{aligned} \quad (7)$$

where  $h_a(x, z)$  is a piecewise linear function,

$$h_a(x, z) = \begin{cases} g(x), & |z| \geq c, \\ -g(x), & |z| \leq c, \end{cases} \quad (8)$$

with  $c > 0$  and

$$g(x) = m_1 x + \frac{1}{2}(m_0 - m_1)(|x + 1| - |x - 1|). \quad (9)$$

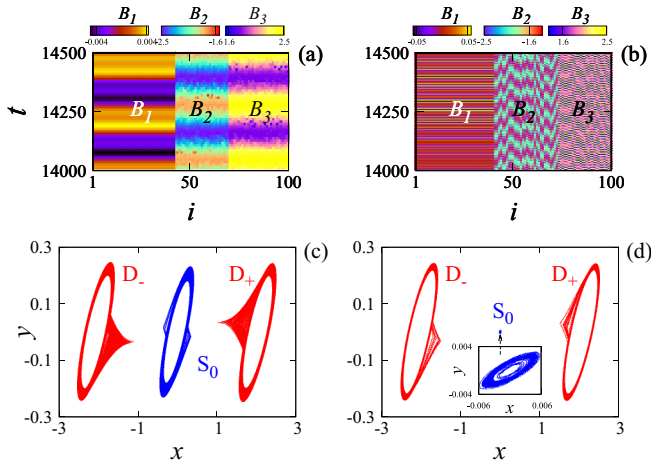


FIG. 8. Chimeric behavior in an ensemble of three-scroll Chua oscillators coupled globally [(a) and (c)] and when driven by a common external noise [(b) and (d)]. Here one synchronized attractor ( $S_0$ ) coexists with two desynchronized attractors ( $D_-$  and  $D_+$ ). The time evolution of 100 oscillators for the two cases is shown in the upper panel with one synchronized group denoted by  $B_1$  and two desynchronized groups  $B_2$  and  $B_3$ . The attractors corresponding to the synchronized ( $S_0$ ) and desynchronized ( $D_-$  and  $D_+$ ) groups are shown in the lower panel. For the case of global coupling,  $K = 0.03$  and  $\rho = 1.47$ , while for the driven case, noise strength  $\varepsilon = 0.5$  and  $\rho = 1$ . Other parameters are  $\alpha = 10$ ,  $\delta = 14$ ,  $c = 1$ ,  $m_0 = -0.43$ , and  $m_1 = 0.41$ . The initial conditions  $x_0, y_0, z_0$  for Chua oscillators are taken randomly in the interval  $[-1, 1]$ .

The coupling affects the parameter  $\rho$ , and for appropriate  $K$  the system is driven to a regime where a synchronized attractor coexists with two desynchronized attractors. This system evolves to a chimera, where a synchronized group (marked as  $B_1$ ) coexists with two desynchronized groups (marked as  $B_2$  and  $B_3$ ), as shown in Fig. 8(a). The dynamics of the oscillators in the synchronized group is on the attractor  $S_0$ , and the desynchronized oscillators can settle either on attractor  $D_-$  or  $D_+$  shown in Fig. 8(c). Similar chimeric behavior is observed when the ensemble is driven by a common external signal,  $f(t)$ . For numerical illustration, we consider  $f(t)$  to be Gaussian white noise with mean 0 and standard deviation 0.01. The resulting chimeras with synchronized group ( $B_1$ ) and desynchronized groups ( $B_2$  and  $B_3$ ) with the corresponding attractors are shown in Figs. 8(b) and 8(d). It should be noted that unlike the case of Lorenz oscillators where both coupling and forcing can induce chimeras irrespective of the variable in which the coupling is introduced [32], for Chua oscillators chimeras can only be observed when the oscillators are coupled in  $y$ . This is because the Lorenz oscillator can show multistability (coexisting fixed points and attractor) if any of the system parameters  $\sigma$ ,  $r$ , or  $\beta$  is varied, whereas an isolated Chua system is multistable with respect to changes in  $\rho$  only.

#### IV. SUMMARY

In this work, we have examined the emergence of dynamical chimeras in ensembles of coupled chaotic oscillators, and in

the absence of explicit nonuniformity in the coupling. The symmetry-breaking that leads to robust chimeric dynamics occurs due to two features: Multistability is induced in the system *through* the coupling, and the basins of the different attractors are intertwined in a complicated structures. It should be mentioned here that chimera-like states can be observed even when the basins of coexisting attractors are not intermingled, but when multistability and intertwined basins are present together, the system inevitably shows robust chimeras that can be realized even for small system sizes. Therefore, although each of these features was discussed separately earlier, drawing on them together ensures that one can design chimeras with desired features. Furthermore, an ensemble of identical chaotic oscillators (that may or may not be coupled to each other) when driven by a common external signal can also have chimeras; this observation may be of considerable significance.

The attractors on which the synchronized motion occurs are very different from the original strange attractor, and they appear due to the stabilization of the fixed points when the parameters are modified because of the diffusive nature of the coupling. Moreover, these chimeras can be observed with global coupling alone (namely without driving) for appropriate parameter values. It should be emphasized that although the results presented here are for Lorenz oscillators driven by common Gaussian noise, similar states can be observed in other double or multiscroll response systems [34,35] and for other forms of driving (chaotic, quasiperiodic, periodic, etc.).

Our results show that even common background noise is sufficient to observe chimeric behavior. There are biological and physical examples in which chaotic dynamics is undesirable and one needs the entire or part of the system to switch to regular dynamics [7,36]. Since in many such systems, especially biological systems, it is not possible to change the system parameters, one can employ a forcing technique to bring the effective parameters to the desired values [37]. For example, in diseases such as epilepsy and Parkinson's disease, control strategies such as forcing can be used to switch the brain dynamics to the desired state. Studies have found that background white noise can improve cognitive functioning in individuals in hypo-dopaminergic states or with ADHD [38]. Such forcing techniques can also be used for the successful operation of power grid networks and to avoid grid failures. We believe that the present results can therefore have wide applicability in different areas of science and technology.

#### ACKNOWLEDGMENTS

R.R. acknowledges the Department of Science and Technology for support through the J. C. Bose National Fellowship. A.P. and N.P. thank Department of Science and Technology, India. N.P. acknowledges Max Planck Institute for the Physics of Complex Systems for research support. S.R.U. is thankful to CSIR India for financial support through the award of Senior Research Fellowship.

- [1] Y. Kuramoto and D. Battogtokh, *Nonlinear Phenom. Complex Syst. (Minsk, Belarus)* **5**, 380 (2002).
- [2] D. M. Abrams and S. H. Strogatz, *Phys. Rev. Lett.* **93**, 174102 (2004).
- [3] A. E. Motter, S. A. Myers, M. Anghel, and T. Nishikawa, *Nat. Phys.* **9**, 191 (2013).
- [4] F. Dorfler, M. Chertkov, and F. Bullo, *Proc. Natl. Acad. Sci. (U.S.A.)* **110**, 2005 (2013).
- [5] N. C. Rattenborg, C. J. Amlaner, and S. L. Lima, *Neurosci. Biobehav. Rev.* **24**, 817 (2000).
- [6] C. R. Laing and C. C. Chow, *Neural Comput.* **13**, 1473 (2001); C. R. Laing, W. C. Troy, B. Gutkin, and G. B. Ermentrout, *SIAM J. Appl. Math.* **63**, 62 (2002).
- [7] M. J. Panaggio and D. M. Abrams, *Nonlinearity* **28**, R67 (2015).
- [8] G. C. Sethia, A. Sen, and F. M. Atay, *Phys. Rev. Lett.* **100**, 144102 (2008).
- [9] A. Yeldesbay, A. Pikovsky, and M. Rosenblum, *Phys. Rev. Lett.* **112**, 144103 (2014).
- [10] S. R. Ujjwal and R. Ramaswamy, *Phys. Rev. E* **88**, 032902 (2013); S. R. Ujjwal, N. Punetha, and R. Ramaswamy, *ibid.* **93**, 012207 (2016).
- [11] C. R. Laing, K. Rajendran, and I. G. Kevrekidis, *Chaos* **22**, 013132 (2012).
- [12] J. H. Sheeba, V. K. Chandrasekar, and M. Lakshmanan, *Phys. Rev. E* **79**, 055203(R) (2009).
- [13] H. Sakaguchi, *Phys. Rev. E* **73**, 031907 (2006).
- [14] C. R. Laing, *Phys. Rev. E* **81**, 066221 (2010).
- [15] N. Punetha, S. R. Ujjwal, F. M. Atay, and R. Ramaswamy, *Phys. Rev. E* **91**, 022922 (2015).
- [16] G. C. Sethia and A. Sen, *Phys. Rev. Lett.* **112**, 144101 (2014).
- [17] M. Wolfrum and O. E. Omel'chenko, *Phys. Rev. E* **84**, 015201(R) (2011).
- [18] M. Wolfrum, O. E. Omel'chenko, S. Yanchuk, and Y. L. Maistrenko, *Chaos* **21**, 013112 (2011).
- [19] V. K. Chandrasekar, R. Suresh, D. V. Senthilkumar, and M. Lakshmanan, *Europhys. Lett.* **111**, 60008 (2015).
- [20] A. Pikovsky, M. Rosenblum, and J. Kurths, *Synchronization: A Universal Concept in Nonlinear Sciences* (Cambridge University Press, Cambridge, 2001).
- [21] E. Ott, J. C. Alexander, I. Kan, J. C. Sommerer, and J. A. Yorke, *Physica D* **76**, 384 (1994).
- [22] E. N. Lorenz, *J. Atmos. Sci.* **20**, 130 (1963).
- [23] L. M. Pecora and T. L. Carroll, *Phys. Rev. Lett.* **64**, 821 (1990).
- [24] S. Guan, C. H. Lai, and G. W. Wei, *Phys. Rev. E* **71**, 036209 (2005); S. Guan, Y. C. Lai, and C. H. Lai, *ibid.* **73**, 046210 (2006); M. Agrawal, A. Prasad, and R. Ramaswamy, *ibid.* **87**, 042909 (2013).
- [25] C. Sparrow, *The Lorenz Equations: Bifurcations, Chaos and Strange Attractors* (Springer, New York, 1982).
- [26] S. H. Strogatz, *Nonlinear Dynamics and Chaos: With Applications to Physics, Biology, Chemistry, and Engineering* (Perseus Books, New York, 1994).
- [27] S. Camargo, R. L. Viana, and C. Anteneodo, *Phys. Rev. E* **85**, 036207 (2012).
- [28] T. W. Tanze, S. R. Ujjwal, and R. Ramaswamy (unpublished).
- [29] N. F. Rulkov, M. M. Sushchik, L. S. Tsimring, and H. D. I. Abarbanel, *Phys. Rev. E* **51**, 980 (1995).
- [30] M.-L. Chabanol, V. Hakim, and W.-J. Rappel, *Physica D* **103**, 273 (1997).
- [31] O. E. Röessler, *Phys. Letts. A* **57**, 397 (1976).
- [32] We have shown the results when the drive is given in  $z$ -variable only; qualitatively similar chimeras can be observed when coupling is in  $x$ - or  $y$ -variable or even in the case when driving is given in all three variables [28]. In all these cases, the mechanism that drives the system into multistability is similar but affects different parameters of the system depending upon in which direction the system is forced.
- [33] S. R. Ujjwal, N. Punetha, R. Ramaswamy, M. Agrawal, and A. Prasad, *Chaos* **26**, 063111 (2016).
- [34] Z. Elhadj and J. C. Sprott, *Int. J. Bifurcation Chaos* **20**, 135 (2010).
- [35] A. M. Rucklidge, *J. Fluid Mech.* **237**, 209 (1992).
- [36] S. Boccaletti, J. Kurths, G. Osipov, D. L. Valladares, and C. S. Zhou, *Phys. Rep.* **366**, 1 (2002).
- [37] A. N. Pisarchik and U. Feudel, *Phys. Rep.* **540**, 167 (2014), and references therein.
- [38] G. B. W. Söderlund, S. Sikström, J. M. Loftesnes, and E. J. Sonuga-Barke, *Behav. Brain Func.* **6**, 1 (2010).